A&A 518, A5 (2010)
DOI: 10.1051/0004-6361/200913462
© ESO 2010

Astronomy & Astrophysics

The role of magnetic reconnection on jet/accretion disk systems

E. M. de Gouveia Dal Pino[1], P. P. Piovezan[1,2], and L. H. S. Kadowaki[1]

[1] Universidade de São Paulo, IAG, Rua do Matão 1226, Cidade Universitária, São Paulo 05508-900, Brazil
e-mail: dalpino@astro.iag.usp.br
[2] Max Planck Institute for Astrophysics, Karl-Schwarzschild-Str. 1, Postfach 1317, 85741 Garching, Germany

Received 13 October 2009 / Accepted 25 April 2010

ABSTRACT

Context. It was proposed earlier that the relativistic ejections observed in microquasars could be produced by violent magnetic reconnection episodes at the inner disk coronal region (de Gouveia Dal Pino & Lazarian 2005).
Aims. Here we revisit this model, which employs a standard accretion disk description and fast magnetic reconnection theory, and discuss the role of magnetic reconnection and associated heating and particle acceleration in different jet/disk accretion systems, namely young stellar objects (YSOs), microquasars, and active galactic nuclei (AGNs).
Methods. In microquasars and AGNs, violent reconnection episodes between the magnetic field lines of the inner disk region and those that are anchored in the black hole are able to heat the coronal/disk gas and accelerate the plasma to relativistic velocities through a diffusive first-order Fermi-like process within the reconnection site that will produce intermittent relativistic ejections or plasmons.
Results. The resulting power-law electron distribution is compatible with the synchrotron radio spectrum observed during the outbursts of these sources. A diagram of the magnetic energy rate released by violent reconnection as a function of the black hole (BH) mass spanning 10^9 orders of magnitude shows that the magnetic reconnection power is more than sufficient to explain the observed radio luminosities of the outbursts from microquasars to low luminous AGNs. In addition, the magnetic reconnection events cause the heating of the coronal gas, which can be conducted back to the disk to enhance its thermal soft X-ray emission as observed during outbursts in microquasars. The decay of the hard X-ray emission right after a radio flare could also be explained in this model due to the escape of relativistic electrons with the evolving jet outburst. In the case of YSOs a similar magnetic configuration can be reached that could possibly produce observed X-ray flares in some sources and provide the heating at the jet launching base, but only if violent magnetic reconnection events occur with episodic, very short-duration accretion rates which are ~100−1000 times larger than the typical average accretion rates expected for more evolved (T Tauri) YSOs.

Key words. acceleration of particles – accretion, accretion disks – black hole physics – magnetic fields – galaxies: jets

1. Introduction

Supersonic jets are observed in several astrophysical systems, such as active galactic nuclei (AGNs), neutron star and black hole X-ray binaries, and low-mass young stellar objects (YSOs), and are probably also associated with gamma-ray bursts. The study of their origin, structure, and evolution helps to shed light on the nature of their compact progenitors, as they carry angular momentum, mass, energy, and magnetic field away from the sources.

The currently most accepted paradigm for jet production is based on the magneto-centrifugal acceleration out of a magnetized accretion disk that surrounds the central source. Firstly proposed by Blandford & Payne (1982; see also Lynden-Bell 1969; Blandford & Rees 1974; and Lovelace 1976, where these ideas initially germinated), this basic scenario for jet launching has been object of extensive analytical and numerical investigation (see e.g., McKinney & Blandford 2009; Shibata 2005; de Gouveia Dal Pino 2005, for reviews). However, though considerable progress has been achieved in the comprehension of the possible origin of the magnetic fields that must permeate the accretion disk and the mechanism of angular momentum transport that allows the accretion to occur through magnetorotational turbulence (Balbus & Hawley 1998), questions related to jet stability, the nature of the coupling between the central source magnetosphere and the disk field lines, and the quasi-periodic ejections that are often associated to these jets, are still debated.

Relativistic jets from stellar-mass black holes of binary stars emitting X-rays, also called microquasar jets (or BHXRB jets), are scaled-down versions of AGN (or quasar) jets, typically extending for ~1 pc and probably powered by the accreting, spinning black hole. Despite the enormous difference in scale, both classes share several similarities in their physical properties. However, because the characteristic times of the matter flow are proportional to the black hole mass, the accretion-ejection phenomena in microquasars end sooner and are about 10^{-7}–10^{-5} faster than analogous phenomena in quasars. This fact and their closer proximity to us (they are generally observable within the Galaxy) make the microquasars easier to investigate compared to the AGNs (Mirabel & Rodrigues 1999).

Although individual systems are complex and peculiar when looked at in detail, there are common features to all classes of BHXRBs (e.g., Remillard & McClintock 2006). According to their X-ray emission (2–20 keV), they show basically two major states: a quiescent and an outburst state. The former is characterized by low X-ray luminosities and hard non-thermal spectra. Usually, transient BHXRBs exhibit this state for long periods, which allows one to obtain the physical parameters of the system as the spectrum of the secondary star becomes prominent.

On the other hand, the outburst state corresponds to intense activity and emission and can be sub-classified in three main active and many intermediary states. According to Remillard & McClintock (2006), the three main active states are the thermal state (TS), the hard state (HS) and the steep power law state

(SPLS). These states are usually explained as changes in the structure of the accretion flow. During the TS, for example, the soft *x*-ray thermal emission comes from the inner region of the thin accretion disk that extends until the last stable orbits around the black hole. On the other hand, during the HS the observed weak thermal component suggests that the disk is truncated at a few hundreds/thousands gravitational radii. The hard X-ray emission measured during this state is often attributed to inverse Compton scattering of soft photons from the outer disk by relativistic electrons in the hot inner region of the system (e.g. Remillard & McClintock 2006; Malzac 2007).

A widely observed example from radio to X-rays is the microquasar GRS 1915+105. Located at a distance of ~12.5 kpc and probably with a 10–18 solar mass black hole in the center of the binary system, it was the first galactic object to show evidence of superluminal radio ejection (Mirabel & Rodrigues 1994; Mirabel & Rodrigues 1998). Dhawan et al. (2000) have distinguished two main radio states of this system, a plateau and a flare state. During the plateau state the RXTE (2–12 keV) soft X-ray emission is weak, while the BATSE (20–100 keV) hard X-rays are strong and the radio flat spectrum is produced by a small scale nuclear jet. On the other hand optically thin ejecta are superluminally expelled up to thousands of AU during the flare phase and the radio spectral index is between 0.5 and 0.8. The soft X-rays also flare during this phase and exhibit a high variability, while the hard X-rays fade for a few days before recovering. In terms of the X-ray spectral states, several works have verified that the radio flares of this source occur during the SPLS (e.g., Fender et al. 2004) and the X-ray emission of both the plateau and the flare state are different manifestations of the SPLS (e.g., Reig et al. 2003).

The examination of radio and X-ray observations for other microquasars (e.g., XTE J1859+226, XTE J1550-564) also suggests that the ejection of relativistic matter happens when the source is very active and in the SPLS (e.g., Hannikeainen et al. 2001; Brocksopp et al. 2002; Fender et al. 2004; McClintock et al. 2007). According to Fender et al. (2004), the origin of the optically thin emission in radio is due to shock waves that are formed in the jet when the system passes from a "hard" SPLS to a "soft" SPLS. However, what generates these shock waves or the triggering mechanism for the ejections of matter is unclear.

In 2005, de Gouveia Dal Pino & Lazarian (see also de Gouveia Dal Pino 2006) proposed a mechanism that can be responsible for the initial acceleration of the plasma jet to relativistic speeds in the case of the microquasar GRS1915+105. Their scenario is related to violent reconnection episodes between the magnetic field lines of the inner disk region and those that are anchored in the black hole. We here revisit this model and argue that it could be responsible for the transition from the "hard" SPLS to the "soft" SPLS seen in other microquasars. We also extend it to the AGN jets and briefly discuss its role for thermal YSO jets (see also de Gouveia Dal Pino 2006; de Gouveia Dal Pino et al. 2009, for earlier discussions).

We note that an interesting correlation between the radio and the (hard) X-ray luminosity has been reported by Laor & Behar (2008) for sources spanning 10^{10} orders of magnitude in mass (from magnetically active stars to some galactic black holes and radio quiet AGNs), and recently extended to dwarf nova outbursts by Soker & Vrtilek (2009). This correlation holds only for sources for which $L_R/L_X < 10^{-5}$ and suggests that a common mechanism may be responsible for the radio emission in these highly different objects. Because in magnetically active stars the emission is related to the coronae, these authors have argued that the same might be occurring in some BHXRBs and radio quiet AGNs, i.e., the radio emission could also come from magnetic activity in the coronae above the accretion disk, just like in the scenario that we investigate here in detail (and which was previously suggested in de Gouveia Dal Pino 2006; de Gouveia Dal Pino et al. 2010a, 2010b).

Earlier studies have also revealed a correlation between the radio and the X-ray luminosity of BHXRBs in their quiescent "low/hard" state and low-luminosity AGNs with nuclear radio emission or weak radio jets (Gallo et al. 2003; Merloni et al. 2003; Falcke et al. 2004)[1].

As also remarked by Soker & Vrtilek, suggestions for the presence of coronae above accretion disks are not new (e.g., Liang & Price 1977; Liang 1979; Galeev et al. 1979; Done & Osborne 1997; Wheatley & Mauche 2005; Cao 2009), and the connection between coronae and jets were previously proposed as well (e.g., Fender et al. 1999; Markoff et al. 2005; de Gouveia Dal Pino & Lazarian 2000, 2001, 2005). If the magnetic activity in erupting accreting disks is similar to that in stars, then coronal mass ejections, as in the Sun, could be expected. Hence magnetic flares similar to those in active stars might be a potential mechanism operating at the jet launching region in a variety of systems, from young stellar objects to BHs (de Gouveia Dal Pino 2006; de Gouveia Dal Pino et al. 2009; Soker 2007; Soker & Vrtilek 2009).

This paper is organized as follows: in Sect. 2 we briefly describe de Gouveia Dal Pino & Lazarian's model. In Sect. 3 we discuss it in the context of the microquasars and in Sect. 4 we propose its generalization to other classes of relativistic jets, extending it to low-luminosity AGN jets. In Sect. 5 we briefly discuss the reconnection model in the context of the YSO jets and finally, in Sect. 6, we draw our conclusions.

2. A simple reconnection scenario in the inner accretion disk/corona region

We consider a magnetized accretion disk around a rotating (Kerr) BH as schematized in Fig. 1. A detailed description of the scenario adopted is given in de Gouveia Dal Pino & Lazarian (2005). Here we briefly present the assumptions made.

A magnetosphere around the central BH may be formed from the drag of magnetic field lines by the accretion disk (e.g., MacDonald et al. 1986; Wang et al. 2002). The disk large-scale poloidal magnetic field could be established by the action of a turbulent dynamo inside the accretion disk (Livio et al. 2003; King et al. 2004; Uzdensky & Goodman 2008) driven, e.g., by the magnetorotational instability (Balbus & Hawley 1998) and disk differential rotation. Although this scenario remains speculative and nothing definitive has been revealed yet by global disk numerical simulations, the action of a turbulent dynamo followed by the advection of the magnetic flux with the gas towards the inner disk region could result in a gradual increase

[1] We notice that these correlations are often interpreted in the context of (advection dominated accretion flow) ADAF models where a geometrically thick and optically thin accretion disk with small mass flow rate is invoked to explain the low/hard X-ray emission accompanied by radio jet activity. In these models a geometrically thin disk structure in the inner region would be recovered when the system switches to a high-accretion flow rate, hence producing a high/soft emission with suppression of the jet activity. In the present model we examine these objects mostly during their outburst phases rather than during their more quiescent states. Besides, because the reconnection mechanism is operating at the interface region between the inner disk and the central source, the choice of a geometrically thin accretion disk (rather than a thick one) is not a crucial point for our model.

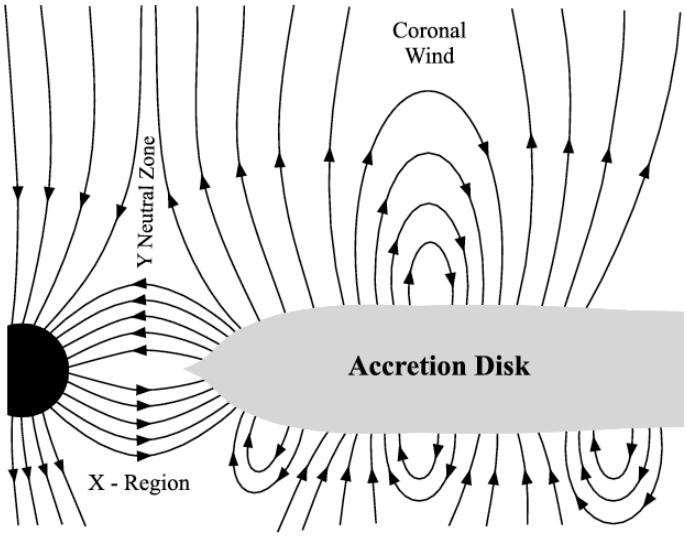

Fig. 1. Schematic drawing of the magnetic field geometry in the inner disk-source region at R_X. From de Gouveia Dal Pino & Lazarian (2005).

of the magnetic flux in this region (e.g., Merloni 2003; Livio et al. 2003; Tagger et al. 2004; de Gouveia Dal Pino & Lazarian 2005; McKinney & Blandford 2009). Even without any dynamo action, a net poloidal field could be built in the inner disk-corona region simply due to advection of existing magnetic flux from the large radii. This has been recently proven to be plausible through three-dimensional numerical simulations (see, e.g., Beckwith et al. 2009, and references therein). These authors have found in particular that most of the magnetic flux inward motion should operate outside the disk body in the coronal region. They found that magnetic stresses driven by differential rotation can create large-scale half-loops of magnetic field that stretch radially inward and then reconnect, leading to discontinuous jumps in the location of magnetic flux. At the end, this mechanism establishes a dipole magnetic field in the inner region with intensity regulated by a combination of magnetic and gas pressures in the inner disk. Although these numerical studies are still preliminary and the saturation condition for this mechanism is not fully understood yet, these results are a demonstration that it is possible to establish a large-scale poloidal field in the inner disk-coronal region.

According to the magneto-centrifugal scenario (Blandford & Payne 1982), this poloidal magnetic flux summed to the disk differential rotation can give rise to a wind that removes angular momentum from the system and increase the accretion rate. This will increase the ram pressure of the accreting material that will then push the magnetic lines in the inner disk region towards the lines which are anchored in the BH horizon allowing a magnetic reconnection event to occur (see the Y-type zone labeled as helmet streamer in Fig. 1). Also, with the accumulation of the poloidal flux in the inner regions the ratio between the gas+radiation pressure to the magnetic field pressure (β) will soon decrease[2]. As we show in Sect. 3.2, when the accretion rate reaches values close to the Eddington limit and $\beta < 1$, the magnetic reconnection event becomes violent and a substantial amount of magnetic energy is released quickly by this process.

If the BH is rotating, closed field lines connecting it with the inner disk edge can lead to angular momentum transfer between them if they are rotating at different angular speeds (Blandford-Znajek 1977). To facilitate the analysis, we consider as in de Gouveia Dal Pino & Lazarian, that the BH and the inner zone of the accretion disk are nearly co-rotating in a way that there is no net angular momentum and energy transfer between them. This is strictly speaking not a necessary condition of the model.

[2] We will see below that β is left as a free parameter in our model, but for violent reconnection events to be produced it must actually decrease to values lower than unity.

3. Revisiting the model: microquasar ejections

We assume here that during the plateau state that precedes a radio flare (e.g., in the microquasar GRS 1915+105) the large scale poloidal field is progressively built in the disk by the dynamo process. Immediately before the flare, the idealized configuration of the system is that of Fig. 1 and both the accretion rate and the magnetic pressure in the inner disk zone become very high due to the reasons described in the preceding section. In order to evaluate the amount of magnetic energy that can be extracted through violent reconnection, we first need to evaluate the physical conditions both in the magnetized disk and in the corona that surrounds it.

3.1. Disk and coronal parameters

Let us assume as in de Gouveia Dal Pino & Lazarian (2005) that the inner radius of the accretion disk (R_X) approximately corresponds to the last stable orbit around the BH. For a BH with stellar mass $M \simeq 14\ M_\odot = M_{14}$ and Schwartzschild radius $R_S = 2GM/c^2 = 4.14 \times 10^6\ M_{14}$ cm (which are parameters suitable for instance for GRS1915+105), this gives $R_X = 3R_S \sim 10^7$ cm.

X-rays observations show that the internal regions of microquasar accretion disks have temperatures higher than $\sim 10^6$ K. At these temperatures, hydrogen, which is probably the main constituent of the disk material, is completely ionized. In this case the main source of disk opacity is the Thomson scattering. Moreover, the thermal pressure of the gas is much less than the radiation pressure and can be neglected. To evaluate the disk quantities at R_X, we adopt the standard model (Shakura & Sunyaev 1973).

In this case, the set of equations that describe a geometrically thin, optically thick, stationary accretion-disk with a Keplerian profile is given by[3]

$$T_d \cong 1,64 \times 10^7 \alpha_{0.5}^{-1/4} M_{14}^{1/8} R_{X,7}^{-3/8} \quad \mathrm{K} \tag{1}$$

$$n_d \cong 3,65 \times 10^{18} \alpha_{0.5}^{-1} M_{14}^{-1/2} \dot{M}_{19}^{-2} R_{X,7}^{3/2} q_{0.82}^{-8} \quad \mathrm{cm}^{-3} \tag{2}$$

$$H_d/R_X \cong 0,57 \dot{M}_{19} R_{X,7}^{-1} q_{0.82}^{4} \tag{3}$$

$$U_d \cong 4,91 \times 10^{14} \alpha_{0.5}^{-1} M_{14}^{1/2} R_{X,7}^{-3/2} \quad \mathrm{erg/cm^3}, \tag{4}$$

[3] We notice that the standard Shakura-Sunyaev model with an α prescription for the viscous stress (which is assumed to be proportional to the total pressure, with α the constant of proportionality) is an idealized simplification of the real physics in accretion disks. When in the radiation dominated regime, it is well known to be subject to thermal and inflow (viscous) instabilities, which make a stationary solution unrealistic. Nonetheless, Hirose and collaborators (see Hirose et al. 2006; Hirose et al. 2009a,b, and references therein), for instance, have recently explored numerically more realistic models, and although they found inconsistencies in the α-models, like for instance that these seem to be actually thermally stable, they could not provide better analytical solutions. We further remark that the real structure of the accretion disk is not a crucial point for the purposes of the present study because the focus is the inner disk-coronal region where the interaction with the central source takes place.

where $\alpha = 0.5\alpha_{0.5}$ is the disk viscosity, $M = 14\ M_\odot M_{14}$, $R_X = 10^7 R_{X,7}$, $\dot{M} = 10^{19}\dot{M}_{19}$ is the disk mass accretion, $q = [1-(R_S/R_X)^{1/2}]^{1/4} = 0.82q_{0.82}$, T_d is the disk temperature, n_d its density, H_d its half-height, and U_d is the photon energy density emitted by the disk.

To determine the accretion rate immediately before an event of violent magnetic reconnection, we assume the equilibrium between the disk gas ram pressure and the magnetic pressure of the magnetosphere anchored at the event horizon of the black hole[4].

Assuming spherical geometry, the radial accretion velocity can be approached by the free fall velocity. Also, assuming that the intensity of the field anchored in the BH horizon is on the order of the inner disk magnetic field (MacDonald et al. 1986; de Gouveia Dal Pino & Lazarian 2005), we find that

$$\frac{3\dot{M}}{4\pi R^2}\left(\frac{2GM}{R}\right)^{1/2} \sim \frac{B_d^2}{8\pi}\,. \tag{5}$$

On the other hand, the disk magnetic field can be parameterized by β, here defined as the ratio between the gas+radiation pressure (which is dominated by the radiation pressure) and the magnetic pressure. Using Eq. (4) to obtain the radiation pressure ($p_d = U_d/3$) and the equation above, we find that the magnetic field and the accretion rate at R_X are

$$B_d \cong 7.54\times 10^7 \beta_{0.8}^{-1/2}\alpha_{0.5}^{-1/2}M_{14}^{1/4}R_{X,7}^{-3/4}\ \ G, \tag{6}$$

$$\dot{M} \sim 1\times 10^{19}\beta_{0.8}^{-1}\alpha_{0.5}^{-1}R_{X,7}\ \ \mathrm{g/s}, \tag{7}$$

where $\beta = 0.8\beta_{0.8}$.

Liu et al. (2002) proposed a simple model to quantify the parameters of the corona of a magnetized disk system. Assuming as in the solar corona that gas evaporation at the foot point of a magnetic flux tube quickly builds up the density of the corona to a certain value and that the tube radiates the heating due to magnetic reconnection through Compton scattering, the coronal temperature and density in terms of the disk parameters can be derived respectively as

$$T_c \cong 4,10\times 10^9\alpha_{0.5}^{-1/8}\beta_{0.8}^{-3/8}M_{14}^{1/16}R_{X,7}^{-3/16}l_{100}^{1/8}\ \ \mathrm{K} \tag{8}$$

$$n_c \cong 5,36\times 10^{15}\alpha_{0.5}^{-1/4}\beta_{0.8}^{-3/4}M_{14}^{1/8}R_{X,7}^{-3/8}l_{100}^{-3/4}\ \ \mathrm{cm^{-3}}, \tag{9}$$

where $l_{100} = 100R_X$ is the scale height of the Y neutral zone in the corona. In the equations above we also assumed that the magnetic field at the reconnection region in the corona is on the order of the field anchored at the disk inner radius (see Fig. 1).

3.2. Rate of magnetic energy released by magnetic reconnection

As described in de Gouveia Dal Pino & Lazarian (2005), the rate of magnetic energy that can be extracted from the Y-zone in the corona (above and below the disk) through reconnection is

$$\dot{W}_B \approx \frac{B^2}{8\pi}v_A(4\pi R_X\Delta R_X), \tag{10}$$

where B is the magnetic field at the reconnection zone, v_A is the coronal Alfvén speed, $v_A = B/(4\pi n_c m_p)^{1/2}$, m_p the hydrogen mass, and ΔR_X is the width of the current sheet. This last term can be estimated considering the condition for which the resistivity at the reconnection zone is anomalous, as in Lazarian & Vishiniac (1999) and de Gouveia Dal Pino & Lazarian (2005):

$$\left(\frac{\Delta R_X}{R_X}\right) \cong 1,86\times 10^{-5}Z^{-1}\alpha_{0.5}^{-3/16}\beta_{0.8}^{7/16}M_{14}^{3/32}R_{X,7}^{-41/32}l_{100}^{11/16}. \tag{11}$$

From Eqs. (6), (10), and (11) we estimate the amount of magnetic energy that can be extracted as

$$\dot{W}_B \cong 1,6\times 10^{35}\alpha_{0.5}^{-19/16}\beta_{0.8}^{-9/16}M_{14}^{19/32}R_{X,7}^{-25/32}l_{100}^{11/16}\ \ \mathrm{erg/s}. \tag{12}$$

The corresponding reconnection time is

$$t_{rec} \cong \frac{R_X}{\xi v_A} \cong 10^{-4}\xi^{-1}R_{X,7}\ \ s, \tag{13}$$

where $\xi = v_{rec}/v_A$ is the reconnection rate and v_{rec} is the reconnection velocity. For the conditions investigated here we find that $v_A \simeq c$.

This relation indicates that for efficient reconnection the release of magnetic energy is very fast, as is that required to produce flares[5]. The energy released could be used to heat the coronal gas (as required by the coronal model; see Eq. (9)) and also to accelerate particles to relativistic velocities, producing a violent radio ejecta (as we will see in the next section).

After reconnection, the destruction of the vertical magnetic flux in the inner disk will increase β, and the corona will return to a less magnetized condition with most of the energy dissipated locally in the disk, instead of in the outflow.

3.3. Particle acceleration and radio emission

According to the discussion in the previous section, we argue that whenever β (the ratio between gas+radiation pressure and magnetic pressure) becomes small enough and the accretion rate attains values near the critical one in the inner disk region, the lines of opposite polarization near the Y-zone will be pressed together by the accreted material sufficiently rapidly as to undergo violent reconnection events. Then energy stored in the magnetic field will be released suddenly and at least part of it will be used to accelerate charged particles. High-speed particles will spew outward, cause the relativistic radio ejecta and produce a luminous blob.

[4] A note is in order here. As remarked in Sect. 2, we assume according to the magneto-centrifugal scenario that the poloidal magnetic flux established in the inner disk region summed to the disk differential rotation can give rise to a wind that removes angular momentum from the system, thus increasing the accretion rate. This will increase the ram pressure of the accreting material (which is continuing to flow from the outer parts of the disk), which will then further push the magnetic lines in the inner disk region towards the lines which are anchored in the BH horizon, allowing a violent reconnection event. Based on this, we can assume the balance between the magnetic pressure and the disk gas ram pressure right before an event of violent reconnection in the inner disk region. On the other hand, without a continuous inflow from the outer disk regions, one might guess that the wind could greatly reduce the amount of accretion flow that reaches the inner disk radius. A similar effect could be achieved also in an ADIOS (adiabatic dominated inflow outflow) model (Blandford & Begelman 1999), which is an ADAF-like solution (Narayan & Yi 1994) with an outflow. However, these are appropriate solutions only for systems that accrete at rates well below the Eddington rate, which is not the case discussed here. Of course, in a real system any of the possibilities above could occur, but in the present study we seek for the best conditions under which a violent reconnection event can be achieved, using a simple analytical description to obtain upper limit estimates for the amount of energy that can be extracted from the reconnection event. Given the non-linearity and intrinsic non-steadiness character of the problem, we hope that future numerical simulations will be able to give us more realistic evaluations.

[5] We note that solar flare observations indicate that the reconnection speed can be as high as a few tenths of the Alfvén velocity (e.g., Takasaki et al. 2004).

de Gouveia Dal Pino & Lazarian (2005) have proposed a mechanism to accelerate particles to relativistic velocities within the reconnection zone in a similar process to the first-order Fermi. Charged particles are confined in the reconnection zone by the particle+magnetic flux coming from both sides of the current sheet in a way that their energies increase stochastically. They have shown that a power-law electron distribution with $N(E) \propto E^{-5/2}$ and a synchrotron radio power-law spectrum $S_\nu \propto \nu^{-0.75}$ can be produced in this case. Kowal, de Gouveia Dal Pino & Lazarian are presently testing this acceleration model in reconnection sites using 3D Godunov-MHD simulations combined with a particle in-cell technique (Kowal et al., in prep.).

This mechanism does not remove the possibility that further out the relativistic fluid may also be produced behind shocks, which are formed by the magnetic plasmons that erupt from the reconnection zone. Behind these shocks a standard first-order Fermi acceleration may also occur resulting a particle power-law spectrum $N(E) \propto E^{-2}$ and a synchrotron spectrum $S_\nu \propto \nu^{-0.5}$. Both radio spectral indices are consistent with the observed spectral range during the flares of GRS 1915-105 ($-0.2 < \alpha_R < -1.0$; Dhawan et al. 2000; Hannikainen et al. 2001).

3.4. X-ray emission

The enhanced X-ray emission that often accompanies the violent flares in microquasars can be easily explained within the scenario presented here as due to the increase in the accretion rate immediately before the violent magnetic reconnection events.

The observed soft X-ray emission is expected to be a fraction of the accretion power, and for an enhanced accretion rate near the Eddington rate this is given by

$$\dot{W}_{ac} \cong \frac{GM_{BN}\dot{M}}{R_X} \cong 1.87 \times 10^{39} M_{14}\dot{M}_{19}R_{X,7}^{-1} \ \ \mathrm{erg/s}, \qquad (14)$$

which is compatible with the soft X-rays observations of Remillard & McClintok (2006). On the other hand, the hard X-ray component, which is also often observed, can be explained by inverse Compton scattering of the soft X-rays photons by the hot electrons of the corona/jet. If this is the case, we expect that after the radio flare the hard X-ray luminosity will decrease because of the decrease of the number of relativistic electrons (because most of them are accelerated away from the system). Indeed, this behavior is also compatible with the observations (e.g. Dhawan et al. 2000).

An estimation of the electrum spectrum at the launching region produced in a magnetic reconnection episode indicates that most of the relativistic electrons should be self-absorbed at this point. When moving away, the produced plasmon cloud dilutes, becoming transparent to its own radiation, first in the infrared and then in radio frequency. The computation of the evolution of this spectrum (e.g., Reynoso & Romero 2009) is out of the scope of the present work as it requires the building of a detailed model for the corona, which will be considered elsewhere. Nonetheless, we can make some predictions by comparing the calculated power released during a violent magnetic reconnection event with the observed luminosities, as below.

3.5. Parameter space

Figure 2 shows a comparison between the calculated magnetic power released during a violent magnetic reconnection event (Eq. (12)) and the observed luminosities for three microquasars with radio jet production, namely GRS1915+105 (a), XTE J1859+226 (b), and XTE J1550-564 (c). The diagram shows the calculated magnetic power released in violent magnetic reconnection events as a function of the central source mass. A suitable choice of the parameter space was used in this calculation: $5\,M_\odot \le M \le 20\,M_\odot$ (e.g., Remillard & McClintock 2006), $0.05 \le \alpha \le 0.5$ (e.g., King et al. 2007), $0.1 \le \beta \le 1$, $1R_S \le l \le 1000R_S$.

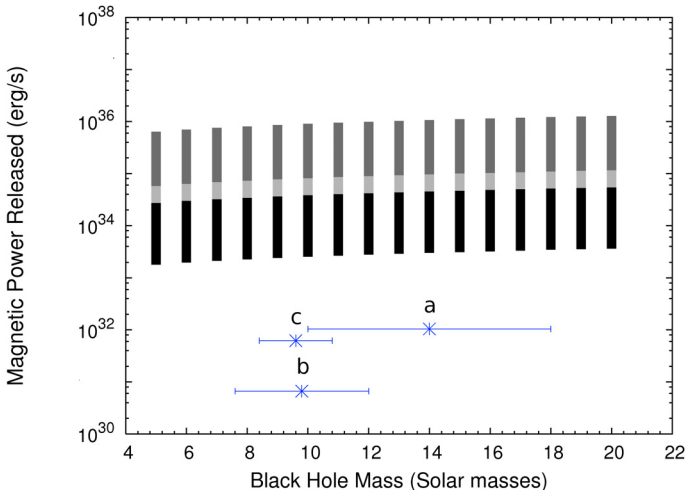

Fig. 2. $\dot{W}_B$ as function of the microquasar black hole mass M. The (blue) stars represent the observed radio luminosities for three microquasars: GRS 1915+105 (a), XTE J1859+226 (b), and XTE J1550-564 (c). The gray scale bars correspond to the calculated magnetic reconnection power and encompasses the parameter space that spans $5M_\odot \le M \le 20\,M_\odot$, $0.05 \le \alpha \le 0.5$, $0.1 \le \beta \le 1$, and $1R_S \le l \le 1000R_S$ (or $0.3R_X \le l \le 333R_X$), with $1R_S \le l \le 10R_S$ in black; $10R_S < l \le 30R_S$ in light gray; and $30R_S < l \le 1000R_S$ in dark gray.

Figure 2 indicates that the magnetic power released by violent magnetic reconnection events is high enough to explain the radio flare luminosities and just marginally high enough to account for the IR luminosity (which has values between 10^{34} erg s^{-1} and 10^{36} erg s^{-1}, for the sources XTE J1859+226 (b) and GRS 1915+105 (a), respectively). It is also possible that additional emission results from electrons that were re-accelerated in optically thin regions away from the reconnection zone (behind shock waves along the jet excited by the plasmon clouds, as emphasized above). This idea is supported for instance by IR observations of GRS 1915+105, which indicate a separation between the IR emission and the central source ~0.2 arcsec or ~2500 AU at 12.5 kpc (Sams et al. 1996), i.e., further away from the predicted launching region by the present model (Fig. 2).

Finally, because the magnetic power released by reconnection is much greater than the observed radio luminosity, only a small fraction of this energy is necessary to accelerate particles. Then most of the energy released would be used to heat the coronal and also the disk gas surface (by thermal conduction along the field lines). This supplementary heating could perturb the accretion disk and result in the variability of the soft X-ray emission observed during the flare phase of GRS 1915+105 (Dahwan et al. 2000).

3.6. Transition between states

According to the scenario presented here, Fig. 1 would correspond to the configuration of the system immediately before a radio flare. Thus, this could be the system configuration at the end of the "hard" SPLS and the transition from the "hard" to

the "soft" SPLS would be due to violent magnetic reconnection events between the magnetic field lines of the inner disk region and those that are anchored into the black hole.

It is important to emphasize that the physical origin of the hard X-ray emission in the SPLS is yet controversial in the literature. Most models claim for the inverse Compton scattering as the dominant radiative mechanism (e.g. Zdziarski 2000), and photons with MeV energies suggest that the scattering occurs in a non-thermal corona (e.g. Zdziarski 2001). For Poutanen & Fabian (1999), the origin of scattering electrons could be the coronal active magnetic regions that rise from the disk, which agrees with the scenario proposed here. Furthermore, the SPLS tends to dominate the spectrum of the BHXRBs as the luminosity reaches values near the Eddington rate, which also agrees with the model presented here.

4. Generalizing the model: AGNs ejections

Despite the huge difference in scales, AGNs/quasars and microquasars have similar morphologies (Mirabel & Rodrigues 1998). Indeed, some studies indicate that the similarity between these systems is more than morphological: they are possibly subject to the same physical processes (e.g., de Gouveia Dal Pino 2005, and references therein for a review). If this is the case, then a generalization of the above scenario to the extragalactic sources is almost straightforward. Indeed, relativistic jets from AGNs are also observed to produce relativistic episodic ejections that originate synchrotron power-law spectrum with similar spectral indices as above.

Considering the same assumptions presented above, we obtain similar scaling relations for AGNs. Figure 3 depicts a synthesis of the generalization of the magnetic reconnection scenario for relativistic sources including both microquasars and AGNs. The diagram shows the calculated magnetic power released in violent magnetic reconnection events as a function of the central source mass. The symbols correspond to the observed radio luminosities of superluminal components (stars for microquasars, circles and triangles for the low luminous AGNs, i.e., LINERs (see below) and Seyfert galaxies, respectively, and squares for luminous AGNs). The same parameter space described in Sect. 3.5 was used for the AGNs, except that the black hole mass now spans the range 5 $M_\odot$ to 10^{10} $M_\odot$.

Figure 3 indicates that the magnetic power released during violent reconnection events is able to explain the emission of relativistic radio blobs from both microquasars and the so-called low-luminous AGNs (LLAGNs), which include Seyfert galaxies and LINERs (these latter have emission-line luminosities that are typically a factor of 10^2 orders of magnitude smaller than those of luminous AGNs; e.g., Ho et al. 1997). This establishes a correlation between the magnetic reconnection power of stellar mass and supermassive black holes according to Eq. (12) spanning over 10^9 orders of magnitude in mass of the sources.

We notice that a simple power-law dependence of $\dot{W}_B$ with the black hole mass M may be derived from Eq. (12) if we consider that the height of the reconnection zone in the corona, l, is parameterized by R_X, which in turn is $R_X = 3R_S = 6GM/c^2$. This implies that according to the present coronal-disc model, $\dot{W}_B \propto \alpha^{-19/16}\beta^{-9/16}M^{1/2}$, and this explains the approximately straight inclination of the thick gray scale curve of Fig. 3.

This result is consistent with the recently found empirical correlation between the radio and the (hard) X-ray luminosity, mentioned in Sect. 1, for sources spanning from magnetically active stars to some BHXRBs and radio quiet AGNs)

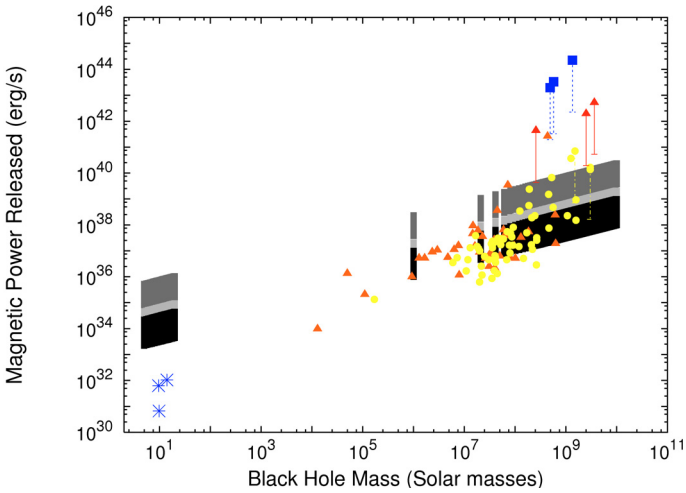

Fig. 3. $\dot{W}_B$ versus the BH mass M for both microquasars and AGNs. The stars represent the observed radio luminosities for the same three microquasars of Fig. 2. The circles, triangles, and squares are observed radio luminosities of jets at parsec scales from LINERS, Seyfert galaxies, and luminous AGNs (or quasars), respectively (obtained from Kellermann et al. 1998; Nagar et al. 2005). The masses of the AGN BHs were evaluated from the central stellar velocity dispersion given by Tremaine et al. (2002). The vertical thin bars associated to some sources stand for a reduction by a factor of 100 in the (isotropic) observed luminosities due to relativistic beaming. The thick bars correspond to the calculated magnetic reconnection power and encompass the parameter space that spans $5M_\odot \leq M \leq 10^{10}\,M_\odot$, $0.05 \leq \alpha \leq 0.5$, $0.1 \leq \beta \leq 1$, and $1R_S \leq l \leq 1000R_S$ (or $0.3R_X \leq l \leq 333R_X$), with $1R_S \leq l \leq 10R_S$ in black, $10R_S < l \leq 30R_S$ in light gray, and $30R_S < l \leq 1000R_S$ in dark gray.

(Laor & Behar 2008; see also Soker & Vrtilek 2009). As remarked before, this correlation clearly suggests that the radio emission in some BHXRBs and low-luminous AGNs comes mainly from magnetic activity in the coronae above the accretion disk and is therefore nearly independent of the intrinsic physics of the central source and the accretion disk, just like in the model above (see also de Gouveia Dal Pino 2006; de Gouveia Dal Pino et al. 2009).

The correlation found in Fig. 3 does not hold for radio-loud AGNs, possibly because their surroundings are much denser and then "mask" the emission due to coronal magnetic activity. In this case, particle re-acceleration behind shocks will probably prevail further out in the jet-launching region and will be the main responsible for the radio emission.

5. In the context of YSOs

Young stellar objects differ in many aspects from microquasars. For instance they produce thermal rather than relativistic jets and exhibit emission lines from which their physical properties (such as density and temperature) are inferred. But they may also exhibit an intense magnetic activity that results in a strong and variable X-ray emission (e.g. Bouvier et al. 2007a,b). Observed flares in X-rays are often attributed to magnetic activity in the stellar corona (Feigelson & Montmerle 1999). However, some COUP (Chandra Orion Ultra-deep Project) sources have revealed strong flares that were related to peculiar gigantic magnetic loops linking the magnetosphere of the central star with the inner region of the accretion disk. It has been argued that this X-ray emission could be due to magnetic reconnection in these gigantic loops (Favata et al. 2005). In this section we examine

this in more detail, investigating the role of magnetic reconnection events in the inner disc/corona of YSOs to explain the X-ray flares and check if magnetic reconnection may be related to the thermal jets of these sources.

We note that previous numerical studies of star-disk interactions have shown that differential rotation between the star and the inner disk regions where the stellar magnetosphere is anchored may lead to field lines opening and reconnection, which eventually restores the initial magnetospheric configuration (e.g., Goodson & Winglee 1999; Matt et al. 2002; Uzdensky et al. 2002; Romanova et al. 2004; von Rekowski & Brandenburg 2004; Zanni 2009; see also Alencar 2007, for a review). Magnetospheric reconnection cycles are expected by most numerical models to develop in a few Keplerian periods at the inner disk, and be accompanied by time dependent accretion onto the star and by episodic outflow events as reconnection takes place. Also, recently several observational results have indicated that the surface magnetic fields of young low-mass stars may be very complex and have high-order multipoles (Valenti & Johns-Krull 2004; Jardine et al. 2006; Daou et al. 2006; Donati et al. 2007). Accretion may then eventually proceed through multipole field lines if the interaction region between star and disk is not very far away from the stellar surface for only the dipole component to be important. This is more likely to happen in stars that present high accretion rates (see below), because them the inner gas disk will extend closer to the star than in the low mass accretion rate systems. Multipolar axisymmetric fields were recently modeled by von Rekowski & Brandenburg (2006). Their time-dependent simulations include a dynamo generated field in the star and the disk and results in a very complex and variable field configuration. In their simulations accretion tends to be irregular and episodic.

To analytically estimate the amount of magnetic power that may be released by violent reconnection in the inner disk-star region we will consider here a most simple geometrical configuration to the problem as in Fig. 1. However, while the inner disk regions of microquasars are dominated by radiation pressure, the inner disk region of YSOs are dominated by gas pressure. Also, instead of modeling the disk/corona of these systems, we used mean values of the coronal density and temperature inferred from observations (Favata et al. 2005) to parameterize our analysis.

The stellar magnetic field is assumed to be quasi dipolar in a way that at R_X this field is given by[6]

$$B_X = \mu B_* \left(\frac{R_*}{R_X}\right)^3 , \tag{15}$$

where B_* is the magnetic field on the surface of the star, R_* is the stellar radius and μ, which is expected to assume values slightly higher than 1, is a parameter that accounts for small deformations of the dipole geometry due to the disk ram pressure (e.g. Shu et al. 2004).

From the equilibrium between the stellar magnetic pressure and the disk ram pressure in the inner disk region we define the radius at which the disk is truncated (e.g., Bouvier et al. 2007b). With these assumptions, the maximum possible accretion rate is reached when the disk touches the stellar surface and can be estimated by

$$\dot{M}_{\rm max} = 1.12 \times 10^{22}\, (\mu B_*)^2_{5000}\, R_2^{5/2} M_1^{-1/2} \qquad {\rm g/s}, \tag{16}$$

where $(\mu B_*) = 5000\,(\mu B_*)_{5000}$ G, $R_* = 2R_\odot R_2$, and $M_* = 1\ M_\odot M_1$ is the stellar mass. These high accretion rates (i.e., around $10^{-4}\ M_\odot$/year) are much higher than the average values estimated for more evolved (class II, classical T Tauri) YSOs ($\simeq 10^{-8}$–$10^{-7}\ M_\odot$/year), but are on the order of the maximum rates expected for younger class I objects, which may undertake FU Ori type outbursts, for example (e.g., Hartmann 2001; Schulz 2005).

Associated to this maximum accretion rate there is a maximum magnetic power released by magnetic reconnection events

$$\dot{W}_{\rm B,\,max} = 1.4 \times 10^{31}\, (\mu B_*)^{-16/7}_{5000}\, M_1^{11/7}\, \dot{M}^{22/7}_{\rm max} R_2^{-48/7} \times n_{11}^{-3/2} T_8^{-1/2} {\rm erg/s}, \tag{17}$$

where $n_c = 10^{11} n_{11}$ cm^{-3} is the coronal density, and $T_c = 10^8 T_8$ K is the coronal temperature (both estimated from observations; Favata et al. 2005).

Figure 4 shows a comparison between the predicted maximum magnetic power released under these circumstances in violent reconnection events and the observed X-ray luminosities (represented by star symbols) for a sample of COUP sources (Favata et al. 2005). The different points associated with each source correspond to different values of (μB_*) (which imply different values of $\dot{M}_{\rm max}$). For most sources, the magnetic power is on the order of (or greater than) the observed luminosities if the maximum accretion rate is $(0.5$–$1)\times 10^{-4}\ M_\odot$/yr (for 10 sources) or $(2.5$–$5)\times 10^{-4}$ (for 5 sources).

These accretion rates of $\sim 10^{-4}\ M_\odot$/yr about 100–1000 times higher than the mean typical rates expected for evolved YSOs would be required only for very short time intervals during violent magnetic reconnection events. This implies that the detection of other spectral signatures of these higher accretion rates would be probably very difficult.

Finally, we argue that the energy released by violent magnetic reconnection processes could help to heat the gas at the base of the jets (Ray et al. 2007). A rough estimate indicates that the large amount of magnetic power released by magnetic reconnection events can be thermally conducted up to distances ~10 AU (Pesenti et al. 2003) on a timescale $\tau_{\rm cond} \sim 10^8 n_{10} T_8^{-5/2} l_{10}^2$ s that is comparable, for instance, to the dynamical timescale of the DGTau jet (e.g., Bacciotti et al. 2002; Cerqueira & de Gouveia Dal Pino 2004).

6. Summary and conclusions

We revisited the model proposed by de Gouveia Dal Pino & Lazarian (2005) for the production of relativistic ejections of microquasar GRS 1915+195. Within this scenario, the initial acceleration of the jet plasma to relativistic speeds is related to violent reconnection episodes between the magnetic field lines of the inner disk region and those that are anchored in the black hole.

[6] We note that Favata et al. (2005), assuming equipartition between gas and magnetic field, have estimated minimum magnetic field values for the loops of the COUP sources that vary between a few dozens to a few kG. On the other hand, the magnetic fields that are typically measured at the surface of (class II) YSOs, i.e., T Tauri stars, are between 1 and 3 kG (e.g., Valenti & Johns-Krull 2004, and references therein; Symington et al. 2005). It is possible that such strong stellar fields are mainly associated with local multipolar components (e.g., starspots) and actually some of these recent polarimetric measurements (Valenti & Johns-Krull 2004) indicate a weaker dipolar component (lower than 200 G). Nonetheless, because, we are concerned with the inner disk-star interacting zone near which the amplitude of the stellar magnetic field must be maximized by the presence of small scale multipoles and compressed field lines, we adopt stellar field magnitudes in the kG range.

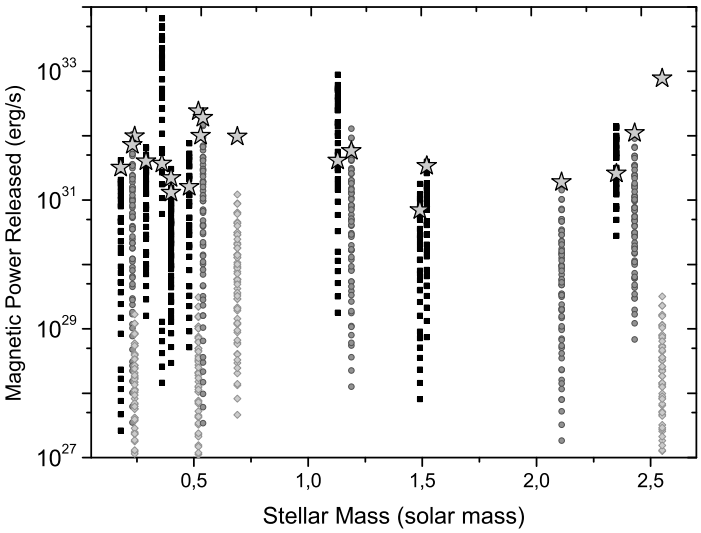

Fig. 4. Magnetic power released by violent magnetic reconnection events for the COUP sources. Each vertical bar corresponds to the calculated magnetic reconnection power for a given source mass, for magnetic fields 1 kG $\leq \mu B_\star \leq (\mu B_\star)_{\max}$ and accretion rates $0.5\dot{M}_{\max} \leq \dot{M} \leq \dot{M}_{\max}$. The lowest magnetic power value of each bar corresponds to $\mu B_\star = 1$ kG and $\dot{M} = 0.5\dot{M}_{\max}$ (Eq. (16)), while the highest magnetic power corresponds to $\mu B_\star = (\mu B_\star)_{\max}$ (Eq. (16)) with $\dot{M}_{\max} = 1 \times 10^{-4} M_\odot$ yr^{-1} (black bars), and $\dot{M}_{\max} = 5 \times 10^{-4} M_\odot$ yr^{-1} (light-gray bars). The stars correspond to the observed X-ray power of the COUP sources (see text for more details).

This might happen whenever a large scale magnetic field (of opposite polarity to that anchored in the BH) arises from the inner accretion disk (probably amplified by dynamo action) so that the ratio between the effective disk pressure and the magnetic pressure (β) decreases to values near 1 or below and the accretion rate ($\dot{M}$) approaches the Eddington rate. In Sect. 3 we extended this model to other microquasars and argued that it could be responsible for the transition from the "hard" SPLS to the "soft" SPLS seen in other microquasars.

In this scenario, the high accretion rate right before a radio flare results in a soft X-ray emission with a luminosity around $\sim 10^{39}$ erg/s (Sect. 3.4). The magnetic power released by violent magnetic reconnection events is mainly used to heat the coronal gas to temperatures of $\sim 10^9$ K (see Eq. (8)) and heat the superficial disk gas by thermal conduction along the field lines causing enhancement and variability of the soft X-ray flux (Sect. 3.5). A substantial fraction of $\dot{W}_B$ is also expected to be used to accelerate particles that produce the relativistic blobs that emit radio-synchrotron-radiation with spectral index of 0.75 if the electrons are first accelerated in the reconnection zone by first-order Fermi like process (Sect. 3.3; de Gouveia Dal Pino & Lazarian 2005). Further out the relativistic fluid may be also re-accelerated behind shocks, which are expected to be formed by the magnetic plasmons that erupt from the reconnection zone. Behind these shocks a standard first-order Fermi acceleration must also produce a synchrotron spectrum $S_\nu \propto \nu^{-0.5}$. Both radio spectral indices are consistent with the observed spectral range during the flares ($\alpha_R \simeq -0.2$ to -1, Dhawan et al. 2000; Hannikainen et al. 2001). The hard X-ray emission is produced by inverse Compton scattering of the soft X-ray emission by the accelerated relativistic electrons and right after a radio flare, the hard X-ray flux should decrease, because most of these electrons are accelerated away from the disk (Sect. 3.4).

In Sect. 4 we generalized this model to AGNs. We built a diagram that compares the calculated power released during violent magnetic reconnection versus the sources black hole masses with the observed outburst radio emission from microquasars and AGNs (Fig. 3). The results indicate that the coronal magnetic activity near the jet launching region can explain the observed emission of relativistic radio blobs from microquasars to low-luminous AGNs (LLAGNs), spanning over 10^9 orders of magnitude in mass of the sources. This correlation does not hold for radio-loud AGNS. These would require reconnection events with super-Eddington accretion to explain the formation and emission of relativistic blobs as due to reconnection. This is possibly because their surroundings are much denser and then "mask" the emission due to coronal magnetic activity at sub-Eddington rates. In this case, particle re-acceleration behind shocks will probably prevail further out in the jet launching region and will be responsible for the radio emission.

A similar magnetic reconnection model applied to the jet launching region of YSO jets suggests that the observed X-ray flares in the sample of COUP sources (Favata et al. 2005) could be explained by violent magnetic reconnection events in the magnetosphere-inner disk coronal region only if high episodic accretion rates are achieved with $\mathrm{d}M/\mathrm{d}t \simeq 100$–$1000\langle \mathrm{d}M/\mathrm{d}t\rangle$ and the inner disk radius approaches the stellar radius during these events. These high accretion rates, however, would last only very briefly, i.e., not for times much longer than the typical reconnection time (Eq. (13)).

We also note that the predicted range of values for the magnetic reconnection power of YSOs naturally lies in the left inferior part of the magnetic reconnection power versus source mass diagram of Fig. 3. This is consistent with the interpretation that the emission processes investigated above in all these classes of sources would be mainly associated with magnetic activity in the coronae and therefore would be nearly independent of the intrinsic physics of the central source and the accretion disk.

Finally, we remark that the simple analytical study carried out here has allowed us to derive estimates of the maximum amount of energy that can be released from violent magnetic reconnection events in the inner region of several accretion disk-coronal-jet systems, as well as its potential effects on these systems, but this is only a first step, and these results must be tested with more realistic multi-dimensional numerical models which are able to capture the intrinsic non-linearity and non-steadiness character of the problem.

Acknowledgements. This work was partially supported by grants of the Brazilian Agencies FAPESP (2006/50654-3) and CNPq and by a grant of the MPIA. The authors acknowledge the useful comments of an anonymous referee.

References

Alencar, S. H. P. 2007, in Star-Disk Interaction in Young Stars, Proc. IAU Symp., 243, 71
Bacciotti, F., Ray, T. P., Mundt, R., Eislöffel, J., & Solf, J. 2002, ApJ, 576, 222
Balbus, S. A., & Hawley J. F. 1998, RvMP, 70, 1
Beckwith, K., Hawley, J. F., & Krolik, J. H. 2009, ApJ, 707, 428
Blandford, R. D., & Beelman, M. C. 1999, MNRAS, 303, L1
Blandford, R. D., & Payne, D. G. 1982, MNRAS, 199, 883
Blandford, R. D., & Rees, M. J. 1974, MNRAS, 169, 395
Blandford, R. D., & Znajek, R. L. 1977, MNRAS, 179, 433
Bouvier, J., Alencar, S. H. P., Boutelier, T., et al. 2007a, A&A, 463, 1017
Bouvier, J., Alencar, S. H. P., Harries T. J., Johns-Krull C. M., & Romanova M. M. 2007b, Protostars and Planets V, 479
Brocksopp, C., Fender, R. P., McCollough, M., et al. 2002, MNRAS, 331, 765
Cao, X. 2009, MNRAS, 2009, 394, 207
Daou, A. G., Johns-Krull, C. M., & Valenti, J. A. 2006, AJ, 131, 520
Cerqueira, A. H., & de Gouveia Dal Pino, E. M. 2004, A&A, 426, L25

de Gouveia Dal Pino, E. M. 2005, Adv. Space Res., 35, 908
de Gouveia Dal Pino, E. M. 2006, Astronomische Nachrichten, 327, 454
de Gouveia Dal Pino, E. M., & Lazarian, A. 2000, ApJ, 536, L31
de Gouveia Dal Pino, E. M., & Lazarian, A. 2001, ApJ, 560, 358
de Gouveia Dal Pino, E. M., & Lazarian, A. 2005, A&A, 441, 845
de Gouveia Dal Pino, E. M., Piovezan, P., Kowal, & Lazarian, A. 2009, in Protostellar Jets in Context, ed. K. Tsinganos, T. Ray, & S. Mathias (Springer Verlag), 89
de Gouveia Dal Pino, E. M., Piovezan, P., Kadowaki, L. H. S. , Kowal, G., & Lazarian, A. 2010, in XXVII IAU General Assembly, ed. I. F Corbett et al., IAU Highlights of Astronomy, 15, in press
Dhawan, V., Mirabel, I. F., & Rodríguez, L. F. 2000, ApJ, 543, 3735
Done, C., & Osborne, J. P. 1997, MNRAS, 288, 649
Falcke, H., Körding, E., & Markoff, S. 2004, A&A, 414, 895
Favata, F., Flaccomio, E., Reale, F., et al. 2005, ApJs, 160, 469
Feigelson, E. D., & Montmerle, T. 1999, ARA&A, 37, 363
Fender, R. P., Garrington, S. T., McKay, D. J., et al. 1999, MNRAS, 304, 865
Fender, R. P., Belloni, T. M., & Gallo, E. 2004, MNRAS, 355, 1105
Galeev, A. A., Rosner, R., & Vaiana, G. S. 1979, ApJ, 229, 318
Gallo, E., Fender, R. P., & Pooley, G. G. 2003, MNRAS, 344, 60
Goodson, A. P., & Winglee, R. M. 1999, ApJ, 524, 159
Hannikainen, D., Wu, K., Campbell-Wilson, D., et al. 2001, ESA SP, 459, 291
Hartmann L. 2001, in Accretion Processes in Star Formation. Accretion Processes in Star Formation (Cambridge, UK: Cambridge University Press), 237, ISBN 0521785200
Hirose, S., Krolik, J. H., & Stone, J. M. 2006, ApJ, 640, 901
Hirose, S., Blaes, O., & Krolik, J. H. 2009a, ApJ, 691, 16
Hirose, S., Krolik, J. H., & Blaes, O. 2009b, ApJ, 704, 781
Ho, L. C., Filippenko, A. V., & Sargent, W. L. W. 1997, ApJS, 112, 315
Jardine, M., Cameron, A. C., Donati, J.-F., Gregory, S. G., & Wood, K. 2006, MNRAS, 367, 917
Kellermann, K. I., Vermeulen, R. C., Zensus, J. A., & Cohen, M. H. 1998, AJ, 115, 1295
King, A. R., Pringle, J. E., West, R. G., & Livio, M. 2004, MNRAS, 348, 111
King, A. R., Pringle, J. E., & Livio, M. 2007, MNRAS, 376, 1740
Laor, A., & Behar, E. 2008, MNRAS, 390, 847
Lazarian, A., & Vishniac, E. 1999, ApJ, 517, 700
Liang, E. P. T. 1979, ApJ, 234, 1105
Liang, E. P. T., & Price, R. H. 1977, ApJ, 218, 247
Liu, B. F., Mineshige, S., & Shibata, K. 2002, ApJ, 572, L173
Livio, M., Pringle, J. E., & King, A. R. 2003, ApJ, 593, 184
Lovelace, R. V. E. 1976, Nature, 262, 649
Lynden-Bell, D. 1969, Nature, 223, 690
MacDonald, D. A., Thorne, K. S., Price, R. H., & Zhang, X. H. 1986, in Black Holes: The Membrane Paradigm, 120
Malzac, J. 2007 [arXiv:0706.2389], unpublished
Markoff, S., Nowak, M. A., & Wilms, J. 2005, ApJ, 635, 1203
Matt, S., Goodson, A. P., Winglee, R. M., & Böhm, K.-H. 2002, ApJ, 574, 232
McKinney, J. C., & Blandford, R. D. 2009, MNRAS, 394, 126
Merloni, A. 2003, MNRAS, 341, 1051
Merloni, A., Heinz, S., & di Matteo, T. 2003, MNRAS, 345, 1057
Mirabel, I. F., & Rodríguez, L. F. 1994, Nature, 371, 46
Mirabel, I. F., & Rodríguez, L. F. 1998, Nature, 392, 673
Mirabel, I. F., & Rodríguez, L. F. 1999, ARA&A, 37, 409
Nagar, N. M., Falcke, H., & Wilson, A. S. 2005, A&A, 435, 521
Narayan, R., & Yi, I. 1994, ApJ, 428, L13
Pesenti, N., Dougados, C., Cabrit, S., et al. 2003, A&A, 410, 155
Poutanen, J., & Fabian, A. C. 1999, MNRAS, 306, L31
Price, R. H., & Thorne, K. S. 1986, Black Holes: The Membrane Paradigm, 1
Ray, T., Dougados, C., Bacciotti, F., Eislöffel, J., & Chrysostomou, A. 2007, Protostars and Planets V, 231
Reig, P., Belloni, T., & van der Klis, M. 2003, A&A, 412, 229
Remillard, R. A., & McClintock, J. E. 2006, ARA&A, 44, 49
Reynoso, M. M., & Romero, G. E. 2009, A&A, 493, 1
Romanova, M. M., Ustyugova, G. V., Koldoba, A. V., & Lovelace, R. V. E. 2004, ApJ, 616, L151
Sams, B. J., Eckart, A., & Sunyaev, R. 1996, Nature, 382, 47
Schulz, N. S. 2005, in From Dust To Stars Studies of the Formation and Early Evolution of Stars, Springer-Praxis books in astrophysics and astronomy (Praxis Publishing Ltd), ISBN 3-540-23711-9
Shakura, N. I., & Syunyaev, R. A. 1973, A&A, 24, 337
Shibata, K. 2005, in Magnetic Fields in the Universe: from Laboratory and Stars to Primordial Structures, ed. E. M. de Gouveia Dal Pino, G. Lugones, & A. Lazarian, AIP Conf. Proc., 784, 153
Shu, F., Najita, J., Ostriker, E., et al. 1994, ApJ, 429, 781
Symington, N. H., Harries, T. J., Kurosawa, R., & Naylor, T. 2005, MNRAS, 358, 977
Soker, N. 2007, IAUS, 243, 195
Soker, N., & Dil Vrtilek, S. 2009 [arXiv:0904.0681], unpublished
Tagger, M., Varniére, P., Rodriguez, J., et al. 2004, ApJ, 607, 410
Takasaki, H., Asai, A., Kiyohara, J., et al. 2004, ApJ, 613, 592
Tremaine, S., Gebhardt, K., Bender, R., et al. 2002, ApJ, 574, 740
Uzdensky, D. A., & Goodman, J. 2008, ApJ, 682, 608
Uzdensky, D. A., Königl, A., & Litwin, C. 2002, ApJ, 565, 1191
Valenti, J. A., & Johns-Krull, C. M. 2004, Ap&SS, 292, 619
von Rekowski, B., & Brandenburg, A. 2004, A&A, 420, 17
von Rekowski, B., & Brandenburg, A. 2006, Astron. Nachr., 327, 53
Wang, D. X., Xiao, K., & Lei, W. H. 2002, MNRAS, 335, 65
Wheatley, P. J., & Mauche, C. W. 2005, ASPC, 330, 257
Zanni, C. 2009, in Magnetic Fields in the Universe II: From Laboratory and Stars to the Primordial Universe – Supplementary CD, ed. A. Esquivel, J. Franco, G. García-Segura, E. M. de Gouveia Dal Pino, A. Lazarian, S. Lizano, & A. Raga, RMxAA, Serie de Conferencias, 36, CD284
Zdziarski, A. A. 2000, In Highly Energetic Physical Processes and Mechanisms for Emission from Astrophysical Plasmas, IAU Symp., 185, 153
Zdziarski, A. A., Grove, J. E., Poutanen, J., Rao, A. R., & Vadawale, S. V. 2001, ApJ, 554, L45